ChemComm

Accepted Manuscript

This article can be cited before page numbers have been issued, to do this please use: Y. Zhang, Y. Cui, X. Li, Y. Du, A. Tang and D. Kong, *Chem. Commun.*, 2019, DOI: 10.1039/C9CC03568K.

ROYAL SOCIETY OF CHEMISTRY

rsc.li/chemcomm

View Article Online
DOI: 10.1039/C9CC03568K

COMMUNICATION

Modified exponential amplification reaction (EXPAR) with improved signal-to-noise ratio for ultrasensitive detection of polynucleotide kinase

Received 00th January 20xx,
Accepted 00th January 20xx

DOI: 10.1039/x0xx00000x

Yu-Peng Zhang[a], Yun-Xi Cui[a], Xiao-Yu Li[a], Yi-Chen Du[a], An-Na Tang[a], De-Ming Kong*[ab]

We incorporated a modified exponential amplification reaction (EXPAR) strategy to design a label-free and "one-pot" biosensor for ultrasensitive detection of polynucleotide kinase (PNK). This method was also successfully applied in screening of PNK inhibitors and analysis of endogenous PNK activity at single-cell level.

Exponential amplification reaction (EXPAR) is an isothermal nucleic acid amplification technique with an ultra-high amplification capacity of >10^6 fold in a short time[1]. Because of such great advantages, it has been widely used in the construction of a variety of biosensors for the detection of microRNA[2], nucleic acid[3], DNA methylation[4], and so on[5,6]. However, traditional EXPAR also brings a serious problem -- high background[7,8] because of non-specific fluorescence response of SYBR Green I to primer, template and undesired by-products[9], thus usually giving unsatisfactory results, especially in end-point detection mode. If the primer, template and undesired by-products can fold into double-stranded structures, this drawback might become more serious, which in turn brings difficulties in primer and template design[10]. Therefore, seeking a facile way which can achieve highly sensitive and specific detection might expand applications of EXPAR in biosensing.

Without adding any additional operating steps and using any expensive reagents, we herein reported a facile way to increase the sensitivity and specificity of EXPAR strategy detection, and demonstrated its superiority by successfully applying it in the highly sensitive detection of an important biomarker -- polynucleotide kinase (PNK). PNK is a prominent member of the 5'-kinase family that can catalyse both the phosphorylation of 5'-hydroxyl groups and the removal of 3'-phosphate groups of oligonucleotides[10,11]. This enzyme is involved in several of gene-related bioprocess such as nucleic acid metabolism, DNA replication, DNA repair, and so on[12-16]. The abnormal expression of PNK activity is associated with a variety of diseases, such as Thomson syndrome[17], Werner syndrome[18], neurodegenerative diseases[19] and spinocerebellar ataxia[17]. In addition, it is also a potential target in cancer treatment[20]. Therefore, PNK can be used as an important biomarker of disease diagnosis and prognosis. Because of the great biological and clinical significance, its activity detection has aroused widespread concern. There are many reports on the detection of this kind of enzyme, including bioluminescent[21], electrochemical[22] and fluorescent[23] methods. In spite of their good performances, some of them are time-consuming, complicated to operate, high-cost, and it's frustrating that the detection limits are not satisfactory[24,25].

Herein, we have filled this gap by applying our modified EXPAR in T4 PNK activity detection. We demonstrated that our modification could indeed give obviously decreased background and greatly improved signal-to-noise ratio, thus enabling ultrasensitive assay of the activity of T4 PNK. Moreover, this method could also be used in detecting endogenous T4 PNK activity in a single cancer cell, screening of T4 PNK inhibitors and the evaluation of their inhibitory capacities.

To take advantage of the powerful signal amplification capability of EXPAR, an oligonucleotide (**T&P**, Table S1) containing a 3'-phosphate terminal was used (Scheme 1). **T&P** integrated the functions of primer and template of EXPAR. The primer sequence, located at the 3'-part of **T&P**, was designed as a hairpin structure. The template sequence, located at the 5'-part of **T&P**, contained two regions with identical sequence, and these two regions were linked with 7 nucleotides, whose complimentary sequence can be specifically recognized by nicking endonuclease Nb.BbvCI. Due to the phosphorylation modification, the 3'-end of **T&P** cannot be extended even in the presence of Klenow fragment polymerase (KFP). PNK is a bifunctional enzymes with both 3'-phosphatase and 5'-kinase activities. Most of reported PNK-sensing strategies were designed on the basis of its 5'-kinase activity[21,22,26-28]. In fact, its 3'-phosphatase has a faster catalytic rate than the 5'-kinase[29],

[a] State Key Laboratory of Medicinal Chemical Biology, Tianjin Key Laboratory of Biosensing and Molecular Recognition, Research Center for Analytical Sciences, College of Chemistry, Nankai University, Tianjin, 300071, P. R. China. Fax: (+)86-22-23502458, E-mail: kongdem@nankai.edu.cn.
[b] Collaborative Innovation Center of Chemical Science and Engineering (Tianjin), Tianjin, 300071, P. R. China.

and is more suitable for highly sensitive detection of T4 PNK[30]. In the presence of T4 PNK, the 3'-phosphate group of **T&P** was hydrolyzed to 3'-hydroxyl, thus then serving as the primer to initiate the polymerization extension by KFP, generating an intramolecular DNA duplex. The duplex product was cleaved into two parts by Nb.BbvCI at its recognition site, and the newly generated 3'-OH end was extended again, displacing the downstream fragment (amplification product). With Cycle 1 in Scheme 1, large numbers of amplification products were produced. In turn, the amplification products can bind with unreacted **T&P** (with 3'-phosphate end) to initiate new nicking-polymerization-displacement reactions (Scheme 1, Cycle 2), leading to an exponential amplification reaction.

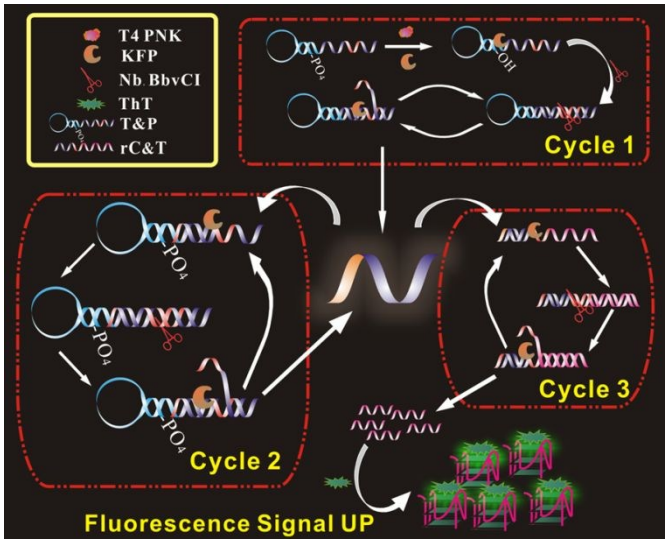

Scheme 1. Working mechanism of modified EXPAR-based T4 PNK-sensing strategy.

To overcome the drawbacks of poor specificity of SYBR Green I-based EXPAR product detection, we introduced an unlabeled oligonucleotide (**rC&T**) in the reaction system. **rC&T** contained two main regions, one was complimentary to above-obtained short-stranded amplification product, the other was a C-rich fragment whose complimentary G-rich sequence can fold into G-quadruplex structure. When **rC&T** was added in the sensing system, the generated single-stranded product might hybridize with **rC&T** strand to initiate another strand displacement amplification reaction (SDA) (Scheme 1, Cycle 3), giving amplified G-rich products which can be sensitively probed by a G-quadruplex-responsive fluorescent probe thioflavin T (ThT). ThT is highly specific towards G-quadruplexes[31,32]. As long as primers, templates and amplification reaction by-products cannot fold into G-quadruplex structures, undesired background will not be generated, ensuring low background. By this way, a modified EXPAR with improved detection sensitivity can be constructed. Since all reaction components can be mixed together before EXPAR reaction, T4 PNK activity-sensing can be performed in a simple "one-pot" mode.

We employed 15% denatured polyacrylamide gel electrophoresis (PAGE) to verify the feasibility of the modified EXPAR-based T4 PNK-sensing strategy. As shown in Fig. 1a, without T4 PNK, neither KFP nor Nb.BbvCI could work on **T&P** strand (Lane 2). After treatment with T4 PNK, however, **T&P** could be extended by KFP to form intramolecular duplex, giving a DNA band (Lane 3) whose migration rate was a little faster than that of **T&P** (Lane 1), indicating that T4 PNK is necessary to initiate the polymerization reaction. With the further addition of Nb.BbvCI, EXPAR can be triggered. Correspondingly, short single-stranded amplification product (Lane 4, in red box), whose migration rate was roughly same as artificially synthesized EXPAR product (Line 9), could be observed. The experimental results strongly suggested that the EXPAR process would be initiated only in the presence of T4 PNK, KFP and Nb.BbvCI all. With the further addition of **rC&T**, both above-mentioned EXPAR product and G-rich product (Lane 7, in red boxes), whose migration rate was identical to that of synthetic G-rich product (Lane 8), were observed, thus demonstrating the feasibility of probing EXPAR reaction using G-quadruplex-specific probes.

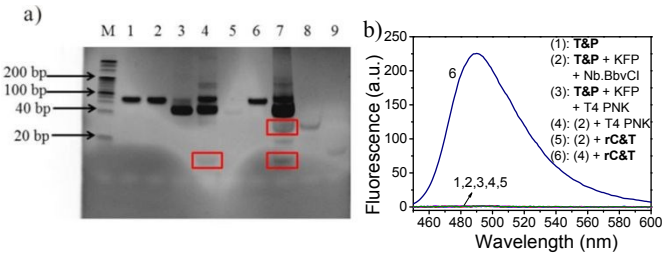

Fig. 1 (a) PAGE analysis of modified EXPAR-based PNK-sensing strategy. (Lane M) DNA marker; (Lane 1) **T&P**; (Lane 2) **T&P** + KFP + Nb.BbvCI; (Lane 3) **T&P** + T4 PNK + KFP; (Lane 4) **T&P** + T4 PNK + KFP + Nb.BbvCI; (Lane 5) **rC&T**; (Lane 6) **T&P** + **rC&T** + KFP + Nb.BbvCI; (Lane 7) **T&P** + **rC&T** + T4 PNK + KFP + Nb.BbvCI; (Lane 8) synthetic G-rich product; (Lane 9) synthetic EXPAR product. (b) Fluorescence spectra of different sensing systems.

We further used fluorescence assay to verify the feasibility of the proposed working mechanism (Fig. 1b). Only in the presence of all important components, including **T&P**, **rC&T**, T4 PNK, KFP and Nb.BbvCI, a significant increase of ThT fluorescence could be observed (Line 6). In the absence of either of the components, however, no detectable fluorescence increase could be observed (Lines 1-5). It should be noted that the sensing system (Line 4) containing **T&P**, T4 PNK, KFP and Nb.BbvCI also gave undetectable fluorescence increase compared to the blank control. In this system, short-stranded EXPAR products could be obtained. But because the products could not fold into G-quadruplexes, ThT would not give corresponding fluorescence response.

In order to achieve the best T4 PNK-sensing performance, some critical experimental conditions were optimized (Fig. S1). Under the optimized conditions (6 nM **T&P**, 160 nM **rC&T**, 1.5 U KFP, 4.5 U Nb.BbvCI and 40 min incubating time), we investigated the analytical capability of the proposed method. As shown in Fig. 2, the fluorescence signal of the sensing system gradually increased in response to increasing concentrations of T4 PNK. In two T4 PNK concentration ranges (5×10^{-6} ~ 0.005 U mL^{-1} and 0.005 ~ 10 U mL^{-1}), good linear correlations between the fluorescence intensity and the logarithm of T4 PNK concentration were observed. The two linear ranges might be related with the two exponential signal amplification steps in the sensing system (Scheme 1, Cycle 2 and Cycle 3) and their

competition for EXPAR product. Based on 3 times standard deviation over the blank response (3δ/slope), the detection limit was estimated to be 1.5×10^{-6} U mL^{-1}, which is the lowest one in the reported T4 PNK activity detection methods as far as our knowledge (Table S2)[17,22,24-27,33,34]. We tried to further simplify the experimental design by changing the template sequence in **T&P** as C-rich sequence, so that **rC&T** will not be needed. However, the obtained **T&P'** (Table S1) gave almost no ThT fluorescence increase even when the reaction time was extended to 3h (Fig. S2). The reason might be that the G-rich amplification product might fold into stable G-quadruplex, thus cannot efficiently trigger exponential EXPAR.

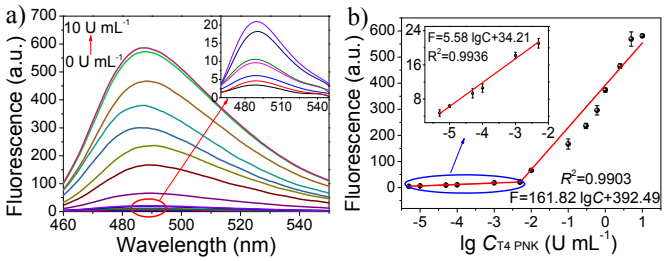

Fig. 2. (a) Fluorescence spectra of the sensing systems containing different amounts of T4 PNK. The insert shows fluorescence spectral change in the range of 5×10^{-6} U mL^{-1}~ 0.005 U mL^{-1} T4 PNK; (b) Linear relationship between the fluorescence intensity at 485 nm and the logarithm of T4 PNK amount.

To demonstrate that our modification can indeed improve the EXPAR-based sensing performance, we compared it with traditional EXPAR using SYBR Green I as the probe for signal detection (Scheme S1). Under the optimized conditions (Fig. S3), this T4 PNK-sensing system gave a linear detection range of 0.04 ~ 0.5 U mL^{-1} with a detection limit of 0.01 U mL^{-1} (Fig. S4), which was about 4 orders higher than that of our modified EXPAR-based sensing system due to the high background from poor recognition specificity and weak response sensitivity of SYBR Green I towards EXPAR products.

We also constructed a SDA-based T4 PNK-sensing platform to highlight the amplification capacity in our sensing method (Scheme S2). Herein, T4 PNK-treated primer **P** plays the identical role to EXPAR product of our modified EXPAR-based sensing system. Because of lacking the amplification by EXPAR, SDA-based T4 PNK-sensing platform gave a detection limit of 1.5×10^{-4} U mL^{-1} under its optimal conditions (Fig. S5 and Fig. S6), which is 2 orders higher than that of our modified EXPAR-based sensing system. Collectively, these experiments demonstrated that the powerful amplification capacity of EXPAR and the excellent G-quadruplex recognition specificity of ThT endow our method with ultra-high detection sensitivity.

Selectivity of biosensors has a huge impact on its practical application potential. Besides ultra-high sensitivity, our method also exhibits good selectivity. As shown in Fig. S7, it could discriminate PNK from other enzymes clearly.

It has been reported that inhibition of PNK activity can be used as a potential means of targeted therapy and can also increase the susceptibility of cancer cells to chemotherapy and radiation therapy[29]. Therefore, the ability to analyze PNK inhibitors has an important significance for the screening of drugs and the development of efficient disease treatment methods[27,29]. To demonstrate the capability of the proposed method for the PNK inhibition assay, we used ammonium sulfate $(NH_4)_2SO_4$ and sodium hydrogen phosphate Na_2HPO_4), two widely studied PNK inhibitors, as the model inhibitors. As depicted in Fig. 3, the relative activity of PNK decreased with the increasing concentrations of $(NH_4)_2SO_4$ and Na_2HPO_4. The obtained IC_{50} values of $(NH_4)_2SO_4$ and Na_2HPO_4 were 7.8 mM and 14.0 mM respectively, which is consistent with previous research[27,30,35], demonstrating that the proposed method can be used to screen PNK inhibitors and evaluate their inhibitory activities, which is of great importance in the development of kinase-targeted drugs.

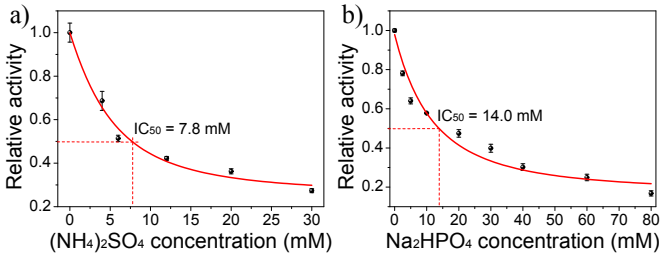

Fig. 3. Relative activity of T4 PNK in the presence of increasing concentrations of (a) $(NH_4)_2SO_4$ and (b) Na_2HPO_4.

To further investigate the potential applications of our proposed method in real biological samples, we detected PNK activity in HeLa cell lysates. As shown in Fig. 4a, addition of HeLa lysates resulted in significant fluorescence enhancement of the sensing system. To verify that the observed fluorescence enhancement was indeed caused by active PNK in the cell lysates, PNK inhibitor $(NH_4)_2SO_4$ and Na_2HPO_4 were added into the cell lysates. As expected, fluorescence output was greatly reduced (As the previous experiment concluded, the inhibition ability of $(NH_4)_2SO_4$ is stronger than Na_2HPO_4). Meanwhile, when the cell lysates were heated at 95 °C for 15 min to deactivate the PNK activity, the heat-treated cell lysates could not cause any detectable fluorescence response at all. These results demonstrated that cell lysates-triggered fluorescence signal enhancement was really related with active PNK. Then, the feasibility of the proposed method for PNK activity quantitation in HeLa cell lysates was investigated. Fig. 4b showed the fluorescence intensities given by the sensing systems containing lysates extracted from different numbers of HeLa cells. It could be seen that the fluorescence given by one cell was clearly discriminated from that of blank control, and the fluorescence intensity was linearly changed with the logarithm of cell number in the ranges of 1 ~ 100 and 100 ~ 2000 cells (Fig. 4c). According to the fluorescence given by the lysates of 2000 cells, the PNK activity in HeLa cells was estimated to be 6.2×10^{-5} U cell^{-1}, which was comparable to that reported in literature[30]. Notably, this method enables sensitive detection of endogenous PNK activity at the single-cell level. What's more, expression levels of PNK activity in normal MDCK (Madin-Darby canine kidney) cells were measured (Fig. 4d). The results showed the PNK activity of cell lysates followed the order of HeLa > MDCK, indicating that cancer cell lines may express more PNK than normal ones. These results suggest that our method has great promise for detecting PNK activity in biological samples, and thus showing great potential in practical applications.

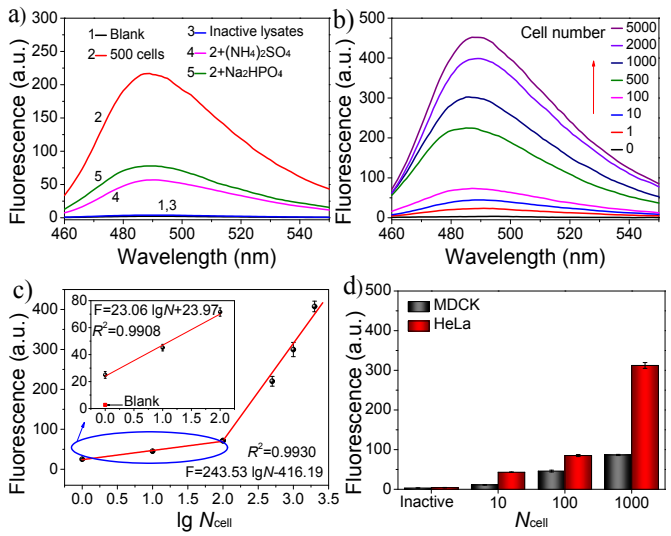

Fig. 4. PNK activity detection in cell lysates. (a) Fluorescence spectra given by different sensing systems. 500 HeLa cells and 25 mM $(NH_4)_2SO_4$ (or Na_2HPO_4) were used; (b) Fluorescence spectra of the sensing systems containing HeLa cell lysates extracted from different amounts of cells; (c) Linear relationship between the fluorescence intensity and the logarithm of cell number. *N* represents the number of HeLa cells; (d) Fluorescence intensities of the sensing systems containing cell lysates extracted from different numbers of MDCK or HeLa cells.

In conclusion, to improve the performance of EXPAR-based biosensors, we reported a modified EXPAR strategy. Compared to the traditional EXPAR using SYBR Green I as the probe, our modified one still follows the label-free detection mode, simple "one-pot" operation (without introducing any additional steps), and shows greatly reduced background, increased fluorescence signal output and thus improved signal-to-noise ratio and detection sensitivity. Such a modified EXPAR strategy was successfully used for the PNK sensor design. The constructed sensing platform achieved an ultra-sensitive detection of T4 PNK activity in a wide concentration range (5×10^{-6} ~ 10 U mL^{-1}) with detection limit of 1.5×10^{-6} U mL^{-1}. Endogenous PNK activity measurement at single-cell level was demonstrated to be possible. What's more, it could also be applied in screening of PNK inhibitors, thus showing great potential applications in drug discovery and clinic diagnosis. We believe that the reported modification strategy might promote the applications of EXPAR in biosensing field.

This work was supported by the National Natural Science Foundation of China (Nos. 21874075, 21728801) and the Fundamental Research Funds for Central University, Nankai University (63191523, 63191728).

Conflicts of interest

There are no conflicts to declare.

Notes and references

1 J. Van Ness, L. K. Van Ness and D. J. Gala, *Proc. Natl. Acad. Sci. U. S. A.*, 2003, **100,** 4504-4509.
2 H. X. Jia, Z. P. Li, C. H. Liu and Y. Q. Cheng, *Angew. Chem. Int. Ed.*, 2010, **49,** 5498–5501.
3 M. Huang, X. Zhou, H. Wang and D. Xing, *Anal. Chem.*, 2018, **90,** 2193-2200.
4 Y. Sun, Y. Sun, W. Tian, C. Liu, K. Gao and Z. Li, *Chem. Sci.*, 2018, **9,** 1344-1351.
5 M. S. Reid, X. C. Le and H. Zhang, *Angew. Chem. Int. Ed.*, 2018, **57,** 11856–11866.
6 Z. Z. Zhang and C. Y. Zhang, *Anal. Chem*., 2012, **84**, 1623-1629.
7 M. S. Reid, R. E. Paliwoda, H. Zhang and X. C. Le, *Anal. Chem.*, 2018, **90,** 11033−11039.
8 J. Chen, X. Zhou, Y. Ma, X. Lin, Z. Dai and X. Zou, *Nucleic Acids Res.*, 2016, 44, e130.
9 G. L. Wang and C. Y. Zhang, *Anal. Chem.*, 2012, **84**, 7037-7042.
10 D. Wang, Y. Chai, Y. Yuan and R. Yuan, *Anal. Chem.*, 2017, **89,** 8951-8956.
11 C. C. Richardson, *Proc. Natl. Acad. Sci. U. S. A.*, 1965, **54,** 158-165.
12 C. J. Whitehouse, R. M. Taylor, A. Thistlethwaite, H. Zhang, F. Karimi-Busheri, D. D. Lasko, M. Weinfeld and K. W. Caldecott, *Cell*, 2001, **104,** 107–117.
13 I. Ahel, D. Ahel, T. Matsusaka, A. J. Clark, J. Pines, S. J. Boulton and S. C. West, *Nature*, 2008, **451,** 81-85.
14 F. Karimi-Busheri, A. Rasouli-Nia, J. Allalunis-Turner and M. Weinfeld, *Cancer Res.*, 2007, **67,** 6619-6625.
15 S. Liu, T. Liu and L. Wang, *Chem. Commun.*, 2015, **51,** 176-179.
16 N. K. Bernstein, R. S. Williams, M. L. Rakovszky, D. Cui, R. Green, F. Karimi-Busheri, R. S. Mani, S. Galicia, C. A. Koch, C. E. Cass, D. Durocher, M. Weinfeld and J. N. Glover, *Mol. Cell*, 2005, **17,** 657-670.
17 H. Zhang, Z. Zhao, Z. Lei and Z. Wang, *Anal. Chem.*, 2016, **88,** 11358-11363.
18 N. Tahbaz, S. Subedi and M. Weinfeld, *Nucleic Acids Res.*, 2012, **40,** 3484-3495.
19 I. Ahel, U. Rass, S. F. El-Khamisy, S. Katyal, P. M. Clements, P. J. McKinnon, K. W. Caldecott and S. C. West, *Nature*, 2006, **443,** 713-716.
20 T. R. Mereniuk, R. A. Maranchuk, A. Schindler, J. Penner-Chea, G. K. Freschauf, S. Hegazy, R. Lai, E. Foley and M. Weinfeld, *Cancer Res.*, 2012, **72,** 5934-5944.
21 J. Du, Q. Xu, X. Lu and C. Y. Zhang, *Anal. Chem.*, 2014, **86,** 8481-8488.
22 L. Cui, Y. Li, M. Lu, B. Tang and C. Y. Zhang, *Biosens. Bioelectron.*, 2018, **99,** 1-7.
23 C. Song and M. Zhao, *Anal. Chem.*, 2009, **81,** 1383-1388.
24 Y. Zhang, C. Liu, S. Sun, Y. Tang and Z. Li, *Chem. Commun.*, 2015, **51,** 5832-5835.
25 L. J. Wang, Q. Zhang, B. Tang and C. Y. Zhang, *Anal. Chem.*, 2017, **89,** 7255-7261.
26 M. Gao, J. Guo, Y. Song, Z. Zhu and C. J. Yang, *ACS Appl. Mater. Inter.*, 2017, **9,** 38356-38363.
27 T. Hou, X. Wang, X. Liu, T. Lu, S. Liu and F. Li, *Anal. Chem.*, 2014, **86,** 884-890.
28 S. Lian, C. Liu, X. Zhang, H. Wang and Z. Li, *Biosens. Bioelectron.*, 2015, **66,** 316-320.
29 X. Li, X. Xu, J. Song, Q. Xue, C. Li and W. Jiang, *Biosens. Bioelectron.*, 2017, **91,** 631-636.
30 X. Y. Li, Y. C. Du, Y. N. Pan, L. L. Su, S. Shi, S. Y. Wang, A. N. Tang, K. Kim and D. M. Kong, *Chem. Commun.*, 2018, **54,** 13841-13844.
31 X. Y. Li, Y. Cui, Y. C. Du, A. N. Tang and D. M. Kong, *ACS Sens.*, 2019, **4,** 1090-1096.
32 Y. C. Du, Y. J. Zhu, X. Y. Li and D. M. Kong, *Chem. Commun.*, 2018, **54,** 682-685.
33 M. Liu, F. Ma, Q. Zhang and C.-Y. Zhang, *Chem. Commun.*, 2018, **54,** 1583-1586.
34 H. N. Chen, Z. H. Wang, X. Chen, K. Lou, A. Z. Sheng, T. S. Chen, G. F. Chen and J. Zhang, *Analyst*, 2019, **144,** 1955-1959.
35 L. Lin, Y. Liu, X. Zhao and J. Li, *Anal. Chem.*, 2011, **83,** 8396-8402.